

# Seasonality of Holocene hydroclimate in the Eastern Mediterranean reconstructed using the oxygen isotope composition of carbonates and diatoms from Lake Nar, central Turkey

Dean, Jonathan R.; Eastwood, Warren

DOI:

[10.1177/0959683617721326](https://doi.org/10.1177/0959683617721326)

License:

None: All rights reserved

*Document Version*

Peer reviewed version

*Citation for published version (Harvard):*

Dean, JR & Eastwood, W 2017, 'Seasonality of Holocene hydroclimate in the Eastern Mediterranean reconstructed using the oxygen isotope composition of carbonates and diatoms from Lake Nar, central Turkey', *The Holocene*. <https://doi.org/10.1177/0959683617721326>

[Link to publication on Research at Birmingham portal](#)

## **Publisher Rights Statement:**

(c) Sage 2017.

Final Version of Record published as above.

## **General rights**

Unless a licence is specified above, all rights (including copyright and moral rights) in this document are retained by the authors and/or the copyright holders. The express permission of the copyright holder must be obtained for any use of this material other than for purposes permitted by law.

- Users may freely distribute the URL that is used to identify this publication.
- Users may download and/or print one copy of the publication from the University of Birmingham research portal for the purpose of private study or non-commercial research.
- User may use extracts from the document in line with the concept of 'fair dealing' under the Copyright, Designs and Patents Act 1988 (?)
- Users may not further distribute the material nor use it for the purposes of commercial gain.

Where a licence is displayed above, please note the terms and conditions of the licence govern your use of this document.

When citing, please reference the published version.

## **Take down policy**

While the University of Birmingham exercises care and attention in making items available there are rare occasions when an item has been uploaded in error or has been deemed to be commercially or otherwise sensitive.

If you believe that this is the case for this document, please contact [UBIRA@lists.bham.ac.uk](mailto:UBIRA@lists.bham.ac.uk) providing details and we will remove access to the work immediately and investigate.

Download date: 25. Apr. 2024

**Dean, J.R.**, Jones, M.D., Leng, M.J., Metcalfe, S.E., Sloane, H.J., Eastwood, W.J., Roberts, C.N., Seasonality of Holocene hydroclimate in the Eastern Mediterranean reconstructed using the oxygen isotope composition of carbonates and diatoms from Lake Nar, central Turkey. *The Holocene* DOI: <https://doi.org/10.1177/0959683617721326>

Copyright © 2017 The authors. Reprinted by permission of SAGE Publications.

**Seasonality of Holocene hydroclimate in the Eastern Mediterranean reconstructed  
using the oxygen isotope composition of carbonates and diatoms from Lake Nar,  
central Turkey**

Jonathan R Dean<sup>1,2,3,4 \*</sup>, Matthew D Jones<sup>2,3</sup>, Melanie J Leng<sup>1,3</sup>, Sarah E Metcalfe<sup>2,3</sup>,  
Hilary J Sloane<sup>1</sup>, Warren J Eastwood<sup>5</sup> and C Neil Roberts<sup>6</sup>

<sup>1</sup>*NERC Isotope Geosciences Facilities, British Geological Survey, UK*

<sup>2</sup>*School of Geography, University of Nottingham, UK*

<sup>3</sup>*Centre for Environmental Geochemistry, University of Nottingham, UK*

<sup>4</sup>*School of Environmental Sciences, University of Hull, UK*

<sup>5</sup>*School of Geography, Earth and Environmental Sciences, University of Birmingham,  
UK*

<sup>6</sup>*School of Geography, Earth and Environmental Sciences, University of Plymouth, UK*

\*Corresponding author Jonathan R Dean

[j.dean2@hull.ac.uk](mailto:j.dean2@hull.ac.uk)

*School of Environmental Sciences, University of Hull, Hull HU6 7RX UK*

## Abstract

A positive shift in the oxygen isotope composition ( $\delta^{18}\text{O}$ ) of lake carbonates in the Eastern Mediterranean from the early to late Holocene is usually interpreted as a change to drier (reduced P/E) conditions. However, it has also been suggested that changes in the seasonality of precipitation could explain these trends. Here, Holocene records of  $\delta^{18}\text{O}$  from both carbonates and diatom silica, from Lake Nar in central Turkey, provide insights into palaeoseasonality. We show how  $\Delta\delta^{18}\text{O}_{\text{lakewater}}$  (the difference between spring and summer reconstructed  $\delta^{18}\text{O}_{\text{lakewater}}$ ) was minimal in the early Holocene and for most of the last millennium, but was greater at other times. For example, between ~4,100-1,600 years BP we suggest that increased  $\Delta\delta^{18}\text{O}_{\text{lakewater}}$  could have been the result of relatively more spring/summer evaporation, amplified by a decline in lake level. In terms of change in annual mean  $\delta^{18}\text{O}$ , isotope mass balance modelling shows that this can be influenced by changes in seasonal P/E as well as inter-annual P/E, but lake level falls inferred from other proxies confirm there was a mid Holocene transition to drier climatic conditions in central Turkey.

## Keywords

Oxygen isotopes; Eastern Mediterranean; lake sediment; Mid Holocene Transition; palaeoseasonality; Turkey

## 1 Introduction

Understanding the detail of hydrological variability over multiple timescales is important in regions such as the Eastern Mediterranean where water stress is increasing (Issar and Adar, 2010) and where management of water supplies under a changing climate is essential (e.g. Kelley et al., 2015). Water availability issues have potentially been critical for societies in the region for millennia (e.g. Weiss et al., 1993) and an understanding of both changes in mean state and seasonality are required (Rohling, 2016). Many studies from the region have shown a shift in the mid Holocene to higher oxygen isotope ratios of lake carbonates ( $\delta^{18}\text{O}_{\text{carbonate}}$ ) (Roberts et al., 2008). These are usually interpreted as responding to changes in the balance between precipitation and evaporation (P/E) (Jones and Roberts, 2008), thus showing a mid Holocene transition from a wetter early Holocene, with relatively more precipitation, to a drier late Holocene, where evaporation losses were relatively increased. However, the extent to which there were shifts in the seasonality of precipitation in the Holocene, and the degree to which these would have affected  $\delta^{18}\text{O}_{\text{carbonate}}$ , remains an unresolved issue in Eastern Mediterranean Holocene palaeoclimatology. Stevens et al. (2001, 2006) suggested that a change from winter- to spring-dominated precipitation was potentially a driver of the increasing  $\delta^{18}\text{O}_{\text{carbonate}}$  trend in the mid Holocene, based on analysis of the sediments of Lakes Zeribar and Mirabad in Iran. Other authors, using pollen and

microcharcoal records, have also argued that there were shifts in the seasonality of precipitation in the region through the Holocene (e.g. Djamali et al., 2010; Turner et al., 2010; Peyron et al., 2011).

Seasonality change analysis requires proxies that are sensitive to different seasons. Dean et al. (2013) showed that comparing  $\delta^{18}\text{O}$  from endogenic carbonates and diatoms at Nar Gölü (Gölü = lake in Turkish) in central Anatolia can provide insights into seasonality as they formed/grew at different times of the year. Such records, combining  $\delta^{18}\text{O}$  from diatoms and carbonates in the same core, remain rare. Here, we present a  $\delta^{18}\text{O}_{\text{carbonate}}$  vs.  $\delta^{18}\text{O}_{\text{diatom}}$  record from Nar Gölü for the entire Holocene, developing a rigorous methodology for diatom isotope data correction, coupled with an isotope mass balance model, to investigate how and why intra-annual variability (seasonality) of  $\delta^{18}\text{O}_{\text{lakewater}}$  changed over time.

## 2 Site description and core material

Nar Gölü (38°20'24''N, 34°27'23''E; 1363 m.a.s.l.; Figure 1) is a maar lake, ~0.6 km<sup>2</sup> in area and >20 m deep, located in the Cappadocia region of central Turkey. The climate of the region is continental Mediterranean (Kutiel and Türkeş, 2005), with precipitation at a nearby meteorological station in Niğde, 45 km from Nar Gölü,

averaging 339 mm per year and peaking in April and May. The crater geology is dominated by basalt and ignimbrite (Gevrek and Kazancı, 2000). The limnology and contemporary sedimentation patterns are described in detail in Dean et al. (2015a), but in summary endogenic carbonate precipitation in the lake surface waters is weighted towards the early summer (end of June/beginning of July), whereas diatom production is weighted towards the spring (end of March/beginning of April). There was ~1.6‰ intra-annual variability in  $\delta^{18}\text{O}_{\text{lakewater}}$  through our June 2011 to July 2012 monitoring period (the period for which we have samples through all seasons), ~0.5‰ of which occurred between the estimated time of peak diatom growth in spring 2012 and carbonate formation in the early summer 2012 (Figure 2). We believe the timing of diatom growth and carbonate precipitation is likely to have stayed roughly the same through the Holocene. As we show in section 4,  $\delta^{18}\text{O}_{\text{lakewater}}$  reconstructed for the time of diatom growth is almost always lower than  $\delta^{18}\text{O}_{\text{lakewater}}$  reconstructed for the time of carbonate precipitation, and this would not be the case if diatom growth was weighted to the summer or early autumn (Figure 2). Indeed, previous work showed there were three planktonic/facultative planktonic ‘bloom’ taxa common in the Nar Gölü diatom record over the last 1,700 years that are likely to have been spring blooming: *Synedra acus*, *Nitzschia palaeacea* and *Cyclotella meneghiniana* (Woodbridge and Roberts 2011). These taxa were also the dominant ‘bloom’ diatoms in the early Holocene (11,700-6,500 years BP) and it is reasonable to assume that their seasonal ecology was

the same at that time as during the late Holocene. The only additional early Holocene bloom diatom is *Aulacoseira ambigua*, but this is only important in two samples (11,657 and 11,403 years BP). In the section from 4,400-3,900 years BP it is possible that *Nitzschia palaea* was a bloom taxon and it is likely to have been spring blooming like *N. palaeacea*. The majority of carbonate is always likely to have precipitated in the early summer in response to increasing evaporation (Dean et al., 2015a).

Figure 1

Figure 2

There have been a number of previous palaeolimnological investigations of the Nar Gölü sediments (e.g. Jones et al., 2006; England et al., 2008; Woodbridge and Roberts, 2010). Here we combine data from the original core sequence taken in 2001/2 (NAR01/02) with new data from a longer core sequence taken in 2010 (Roberts et al., 2016). The chronology of the NAR10 core was constructed by combining varve counting and U-Th dates (Dean et al., 2015b).

### 3 Methods



### 3.1 *Isotope sample preparation and mass spectrometry*

$\delta^{18}\text{O}_{\text{carbonate}}$  data were produced using classic vacuum techniques and an Optima dual-inlet mass spectrometer, as described in detail in Dean et al. (2015b). Specifically, the carbonate analysed for isotopes from the Nar Gölü record was calcite and aragonite, as detailed in Dean et al. (2015b). Data are given as ‰ deviations from VPDB and analytical reproducibility was 0.1‰ for  $\delta^{18}\text{O}$  and  $\delta^{13}\text{C}$ .

Samples for  $\delta^{18}\text{O}_{\text{diatom}}$  analysis need to be as free as possible of non-diatom material since the analytical methods used will liberate oxygen from these other components of the sediment, such as carbonate and detrital silicates. Samples were therefore processed using techniques similar to those of Morley et al. (2004), with the use of hydrogen peroxide, nitric acid (to help remove organics; Tyler et al., 2007), hydrochloric acid, differential settling, sieving at 10  $\mu\text{m}$  and heavy liquid separation stages.  $\delta^{18}\text{O}_{\text{diatom}}$  analysis was carried out on cleaned diatom samples using the stepwise fluorination technique and a Thermo Finnigan MAT 253 at the NERC Isotope Geosciences Facilities. The method is described in Leng and Sloane (2008) and has been verified through an inter-laboratory comparison exercise (Chapligin et al., 2011). The data are presented as ‰ deviations from VSMOW and analytical reproducibility was 0.3‰.

Diatom isotope samples prepared from ~8,800-7,900 and ~4,000-2,350 years BP had insufficient diatom silica for analysis, although there were still diatoms growing in the lake at this time (Roberts et al., 2016).

### 3.2 Correction of diatom isotope data

The samples from Nar Gölü still contained residual detrital silicates after the preparation described above due to a lack of density contrast between the detrital silicates and the diatoms, which reduced the efficacy of heavy liquid separation (Dean et al., 2013). A correction was, therefore, applied to account for the impact of detrital silicates on  $\delta^{18}\text{O}$  (Mackay et al. 2011):

$$\delta^{18}\text{O}_{\text{corrected-diatom}} = (\delta^{18}\text{O}_{\text{diatom}} - \delta^{18}\text{O}_{\text{contamination}} \times [\% \text{contamination} / 100]) / (\% \text{diatom} / 100) \quad (1)$$

where  $\delta^{18}\text{O}_{\text{diatom}}$  is the original isotope value of the prepared diatom sample,  $\% \text{contamination}$  and  $\% \text{diatom}$  are calculated using Eq. 2 (details below) and  $\delta^{18}\text{O}_{\text{contamination}}$  is the isotope value of contamination.

A number of modifications were made to the methodology for the contamination correction of  $\delta^{18}\text{O}_{\text{diatom}}$  samples that was previously used for Nar Gölü sediments (Dean

et al., 2013) to make it more robust. For element concentration data, here we use an XRF (Panalytical epsilon 3 XL) rather than an Energy-Dispersive X-ray Spectroscopy (EDS) probe, allowing for more precise measurements of aluminium concentrations (a good marker for the amount of detrital silicates present (Mackay et al., 2011)), with an analytical reproducibility of 0.03%. The XRF was set up to quantify the proportions of Na, Mg, Al, Si, P, S, K, Ca, Ti, Mn and Fe using the Panalytical Omnia program. Instead of calculating the  $\delta^{18}\text{O}$  of contamination through the intercept of the  $\delta^{18}\text{O}_{\text{diatom}}$  vs. contamination plot, nine turbidites from along the NAR10 core were prepared and run in the same way as the diatom isotope samples. They had a mean  $\delta^{18}\text{O}$  value of 16.0‰ ( $\pm 1.0\text{‰}$ ), which is within uncertainty of the value of 16.5‰ estimated in Dean et al. (2013) from NAR01/02. It is likely that % contamination was overestimated in Dean et al. (2013) because some minerogenic contamination will be removed by the first fluorination stage before  $\delta^{18}\text{O}$  is measured (Swann and Leng, 2009) and diatom frustules can incorporate aluminium, so  $\text{Al}_2\text{O}_3\%$  in the samples does not only reflect minerogenic contamination (Beck et al., 2002; Koning et al., 2007; Swann, 2010; Ren et al., 2013). To investigate the latter effect, Scanning Electron Microscopy (SEM) was used to identify individual clean diatoms (i.e. with no detrital silicates visible at all) and the  $\text{Al}_2\text{O}_3$  wt% of the individual diatoms was measured by EDS, averaging  $1.0\% \pm 0.4$  ( $1\sigma$ ) for the individual diatoms measured across 16 samples. This suggests that there is a significant amount of diatom-bound aluminium, so a correction factor was applied to

account for this. Based on the average  $\text{Al}_2\text{O}_3$  value of the turbidite layers throughout the core sequence that were prepared and run as  $\delta^{18}\text{O}_{\text{diatom}}$  samples, 14.56%  $\text{Al}_2\text{O}_3$  represents 100% contamination (i.e. all detrital silicates, no diatoms). 1‰  $\text{Al}_2\text{O}_3$  represents 0% contamination. Thus, there is an equation, derived from Figure SI-1, that can be used to calculate the new %contamination values for our samples:

$$\%_{\text{contamination}} = (7.3746 \times \text{sample}_{\text{Al}}) - 7.3746 \quad (2)$$

where  $\text{sample}_{\text{Al}}$  is the measured  $\text{Al}_2\text{O}_3$  concentration in each sample analysed for  $\delta^{18}\text{O}_{\text{diatom}}$ . Eq. 2 was used to calculate the %contamination values for Eq. 1. This modified methodology was used on the new samples from NAR10, as well as to recalculate the corrections to the NAR01/02 data presented in Dean et al. (2013). Henceforth,  $\delta^{18}\text{O}_{\text{diatom}}$  refers to the corrected  $\delta^{18}\text{O}_{\text{diatom}}$  data.

Uncertainties from individual components of the correction are outlined in Table 1 and were combined to calculate the overall uncertainty associated with the correction. Uncertainties are reduced compared to those reported in Dean et al. (2013) because of the improved methodology. Figure SI-2 shows the original corrected NAR01/02 data published in Dean et al. (2013) compared to re-calculated values used in this paper. Although the actual values are slightly different and not all of the samples from Dean et

al. (2013) had sufficient material remaining for re-analysis by XRF (so data are now excluded), the general trends are very similar, with periods of lower  $\delta^{18}\text{O}$  particularly at 1,450, 1,250 and 120 years BP. The overall similarities in trends mean that the interpretations of Dean et al. (2013) are still valid, although for consistency in this paper we present the re-analysed NAR01/02 data along with the NAR10 data.

### 3.3 *Calculating $\delta^{18}\text{O}_{\text{lakewater}}$*

To allow for direct comparison of the  $\delta^{18}\text{O}$  data from carbonates and diatoms, we estimate  $\delta^{18}\text{O}_{\text{lakewater}}$  at the time of carbonate precipitation and diatom growth using the calcite (Kim and O'Neil, 1997), aragonite (Grossman and Ku, 1986) and diatom (Crespin et al., 2010) palaeotemperature equations respectively:

$$\delta^{18}\text{O}_{\text{lakewater}} = \delta^{18}\text{O}_{\text{calcite}} - (4.58 \pm [4.58^2 - 4 \times 0.08 \times (13.8 - T)]^{1/2}) / 2 \times 0.08 \quad (3)$$

$$\delta^{18}\text{O}_{\text{lakewater}} = \delta^{18}\text{O}_{\text{aragonite}} - (T - 19.7) / -4.34 \quad (4)$$

$$\delta^{18}\text{O}_{\text{lakewater}} = \delta^{18}\text{O}_{\text{diatom}} - (T - 245) / -6.25 \quad (5)$$

where  $\delta^{18}\text{O}_{\text{lakewater}}$  and  $\delta^{18}\text{O}_{\text{diatom}}$  are expressed on the VSMOW scale,  $\delta^{18}\text{O}_{\text{calcite}}$  and  $\delta^{18}\text{O}_{\text{aragonite}}$  against VPDB and T in °C. We use a temperature range of +15 to +20°C for the time of carbonate precipitation and +5 to +10°C for the time of diatom growth, justified by our measurements of seasonal lake waters from 2011-2013 (Figure 2 and Eastwood et al., unpublished data). The temperature range for the time of diatom growth has been reduced from that used in Dean et al. (2013), where we estimated +5 to +15°C, because of our increased knowledge of intra-annual epilimnion temperature variability with the additional years of temperature logging data from Nar Gölü. While we recognise that there will have been changes in temperature during the Holocene, these changes are likely to have been only a few degrees centigrade (see references in section 5.1), smaller than the ranges of 5°C given for the times of diatom growth and carbonate precipitation.

### 3.4 Lake isotope mass balance models

To examine further the changes in hydroclimate seasonality and how this would be recorded in the seasonality of the lake  $\delta^{18}\text{O}$  system, we use an isotope mass balance model, employing the equations outlined in Jones and Imbers (2010) and Jones et al. (2016), and fully explained in the Supplementary Information. The equations are based on monthly time steps to allow investigations of changing intra-annual  $\delta^{18}\text{O}_{\text{lakewater}}$

variability under different climatic states that have been identified from the isotope data:  
for the present day (Modern), the Mid Holocene (here meaning from approximately  
6,000 to 1,600 years BP) and the Early Holocene.

For the present day, average monthly values of temperature (average [Tav], minimum  
[Tmin] and maximum [Tmax]), total precipitation (P) and snowfall between 2005 and  
2011 (only until 2010 for snowfall) from the meteorological station at Niğde were used  
to drive a model of modern conditions in a lake with the same volume ( $\sim 7,500,000 \text{ m}^3$ )  
and lake area ( $556,500 \text{ m}^2$ ) as Nar Gölü (Table 2 and Supplementary Information).

In this modern lake setting, annual average  $\delta^{18}\text{O}_{\text{lakewater}}$  in the model is 0.59‰ with a  
range (intra-annual  $\delta^{18}\text{O}_{\text{lakewater}}$  variability) of 1.06 (Table 2). This compares to  
measured summer values at Nar Gölü of between  $-1.9$  and  $-0.2$ ‰ for the same period  
(2005-2011), and an intra-annual range of  $\sim 1.6$ ‰ (Dean et al., 2015a). The difference  
between the measured data and the model are due to a number of factors. Firstly, the  
model is for a lake in Niğde, the location of the nearest meteorological station, not for  
Nar Gölü. This will affect the precipitation and evaporation components of the model,  
and therefore the parameterisation of surface and groundwater inflow and outflow,  
which have narrow windows for a given lake in a given location (Jones et al., 2016).  
Nar Gölü is also stratified, adding a level of complexity to the isotope hydrology not

included in the model. However, the model in the Modern scenario has mean and intra-annual  $\delta^{18}\text{O}$  values in the same order as Nar Gölü, and is used here not to recreate conditions at Nar Gölü precisely, but to inform our discussion of why  $\delta^{18}\text{O}$  may change in time. As such, the model is deliberately simple, and appropriate. Inputs to the model for the palaeoclimate scenarios are based on our best understanding of regional temperature and precipitation changes from the literature (see discussions below).

#### 4 Results

Figure 3 shows  $\delta^{18}\text{O}_{\text{carbonate}}$  and  $\delta^{18}\text{O}_{\text{diatom}}$  plotted against depth. There are gaps in both the  $\delta^{18}\text{O}_{\text{carbonate}}$  record, where interpretation of  $\delta^{18}\text{O}_{\text{carbonate}}$  values is complicated by dolomite precipitation (Dean et al., 2015b), and the  $\delta^{18}\text{O}_{\text{diatom}}$  record, because there was not enough diatom silica for isotope analysis and/or samples were too contaminated (with detrital silicates and at times additionally with dolomite), even after cleaning, to run. Because of issues with the chronology discussed elsewhere (Dean et al., 2015b; Roberts et al., 2016), the data between 1034-1161 cm are not plotted on Figure 4.

Figure 3

Figure 4



279

280 The overall trends in  $\delta^{18}\text{O}_{\text{carbonate}}$  and  $\delta^{18}\text{O}_{\text{diatom}}$  are similar. Both have lower values  
 281 towards the bottom of the core in the period likely to be at the time of the Bølling-  
 282 Allerød, higher values at the time of the Younger Dryas, and lower values in the early  
 283 Holocene (Figure 4). Both  $\delta^{18}\text{O}_{\text{diatom}}$  and  $\delta^{18}\text{O}_{\text{carbonate}}$  increase at ~7,500 years BP to  
 284 higher values (by 4‰ VSMOW for  $\delta^{18}\text{O}_{\text{diatom}}$  and ~5‰ VPDB for  $\delta^{18}\text{O}_{\text{carbonate}}$ ).  
 285 However, a major difference is that while there is another increase in  $\delta^{18}\text{O}_{\text{carbonate}}$  (>2‰  
 286 VPDB) ~4,100 years BP, ending with peak Holocene values that are maintained until  
 287 ~1,600 years BP, there is no corresponding second increase in  $\delta^{18}\text{O}_{\text{diatom}}$  values. Where  
 288 data are available,  $\delta^{18}\text{O}_{\text{diatom}}$  values are relatively stable, at c.+37‰ VSMOW for the  
 289 period ~7,000 to 1,600 years BP after rising from early Holocene values of c.+33‰.  
 290 Both  $\delta^{18}\text{O}_{\text{carbonate}}$  and  $\delta^{18}\text{O}_{\text{diatom}}$  decline dramatically at ~1,600 years BP for ~400 years,  
 291 before returning to higher values for most of the last 1,000 years.

292

293 Figure 4 also shows  $\delta^{18}\text{O}_{\text{lakewater}}$  estimated for the times of diatom growth and carbonate  
 294 precipitation. Because late glacial temperatures are not well known, we only use the  
 295 palaeotemperature equations to reconstruct  $\delta^{18}\text{O}_{\text{lakewater}}$  for the Holocene, during which  
 296 annual average temperatures probably only changed by a few degrees in the region (e.g.  
 297 Emeis et al., 2000). The shaded areas on Figure 4C combine maximum and minimum  
 298  $\delta^{18}\text{O}_{\text{lakewater}}$  values possible for the temperature ranges noted above, plus the

uncertainties associated with the  $\delta^{18}\text{O}_{\text{diatom}}$  contamination correction.  $\delta^{18}\text{O}_{\text{lakewater}}$  at the time of diatom growth increased from c. -5‰ in the early Holocene to c. -1‰ in the mid Holocene, before falling to c. -15‰ ~1,600-1,200 years BP and then returning to higher values (c. -2 to -3‰) for the last 1,000 years.  $\delta^{18}\text{O}_{\text{lakewater}}$  at the time of carbonate precipitation increased from c. -3‰ in the early Holocene to c. +1‰ ~6,600 years BP and to c. +3‰ by ~4,000 years BP, before falling to c. -4‰ ~1,600-1,200 years BP and then increasing to c. -1‰ for the last 1,000 years.

$\Delta\delta^{18}\text{O}_{\text{lakewater}}$ , the difference between  $\delta^{18}\text{O}_{\text{lakewater}}$  at the time of carbonate precipitation compared to the time of diatom growth, was only ~1‰ in the early Holocene. It then increased to ~4‰ for much of the time from ~4,100 to 1,600 years BP, as  $\delta^{18}\text{O}_{\text{lakewater}}$  at the time of carbonate precipitation increased 4,100 years BP, but  $\delta^{18}\text{O}_{\text{lakewater}}$  at the time of diatom growth did not (Figure 4C). Then, ~1,600-1,200 years BP, because the fall in  $\delta^{18}\text{O}_{\text{diatom}}$  is much greater than the fall in  $\delta^{18}\text{O}_{\text{carbonate}}$ ,  $\Delta\delta^{18}\text{O}_{\text{lakewater}}$  values are >10‰. For the last 1,000 years,  $\Delta\delta^{18}\text{O}_{\text{lakewater}}$  declined to levels more similar to the early Holocene. Limited variability in recent times is also shown in our monitoring data, with only a 0.5‰ difference in our lakewater samples between April and July in 2012 (Figure 2) and a 0.7‰ difference seen between April and August 2002 (Jones et al., 2005).

## 5 Discussion

From the isotope data, there appear to be three key lake states: 1. limited difference between  $\delta^{18}\text{O}_{\text{lakewater}}$  at the times of diatom growth and carbonate precipitation, i.e.  $\Delta\delta^{18}\text{O}_{\text{lakewater}} \sim 1\text{‰}$  (during the early Holocene and last 1,000 years); 2. intermediate  $\Delta\delta^{18}\text{O}_{\text{lakewater}}$ , at  $\sim 4\text{‰}$  (mid Holocene and up to  $\sim 1,600$  years BP), and 3. maximum  $\Delta\delta^{18}\text{O}_{\text{lakewater}}$ , at  $\sim 10\text{‰}$  ( $\sim 1,600$ - $1,200$  years BP). We discuss these in turn. The differences in resolution between the carbonate and diatom isotope data means that we limit ourselves to comparing the long-term general trends in the data through the early and mid Holocene.

### 5.1 The early Holocene (11,700 to 6,500 years BP)

$\delta^{18}\text{O}_{\text{diatom}}$  and  $\delta^{18}\text{O}_{\text{carbonate}}$  values for the early Holocene are both low relative to the mid and late Holocene (Figure 4), which could indicate higher annual average P/E (i.e. effectively wetter conditions) in the early Holocene, as has been suggested by other studies (summarised in Roberts et al., 2008). Specifically, pollen data (Djamali et al., 2010; Kotthoff et al., 2008; Peyron et al., 2011; Peyron et al., 2017), microcharcoal data (Wick et al., 2003; Turner et al., 2008; Vanniere et al., 2011), climate modelling results (Brayshaw et al., 2010) and  $\delta^{18}\text{O}$  data of freshwater mollusc shells from Çatalhöyük

~160 km SW of Nar (Bar-Yosef Mayer et al., 2012; Lewis et al., 2017) have suggested that the early Holocene in the Eastern Mediterranean region had wetter winters than present, but with many of the studies suggesting drier springs and/or summers. Annual average temperatures were several degrees cooler in the early Holocene compared to the late Holocene, as reconstructed by alkenone-derived sea surface temperatures (Emeis et al., 2000; Triantaphyllou et al., 2009) and speleothem fluid inclusions (McGarry et al., 2004). However, the prominence of *Pistacia* in the pollen record from Nar Gölü (Roberts et al., 2016) and from nearby Eski Acıgöl (Roberts et al., 2001; Woldring and Bottema, 2003), between 11,000 and 8,000 years BP, suggests winters were milder than today (Rossignol-Strick, 1999). Therefore, the inferred drops in annual temperature may have been concentrated in the summer. There is, however, a gap in the  $\delta^{18}\text{O}_{\text{diatom}}$  record between 8,800 and 7,900 years BP due to there being too little diatom silica for diatom isotope measurements to be made. Intriguingly, this period coincides with a phase of marked spring floods on the Çarşamba river in Anatolia (Boyer et al., 2006), which would have been caused by enhanced spring snowmelt in its upper watershed in the Taurus mountains. Despite the fact that spring and summer precipitation may have been lower in the early Holocene than the present day,  $\delta^{18}\text{O}_{\text{carbonate}}$  is still lower in the early Holocene and there is limited  $\Delta\delta^{18}\text{O}_{\text{lakewater}}$ . Presumably, the lower  $\delta^{18}\text{O}_{\text{carbonate}}$  and limited  $\Delta\delta^{18}\text{O}_{\text{lakewater}}$  is due to relatively less summer evaporation of the lake waters compared to the mid and late Holocene, which is to be expected if there were lower

temperatures in the early Holocene spring/summer, as well as increased winter precipitation. Our mass balance modelling allows us to refine our basic interpretation of hydroclimate in the early Holocene.

In our early Holocene model, we have reduced the annual average temperature by 1°C, as estimated from the studies cited above and as used in Jones et al. (2007); details in SI Tables. Annual precipitation values are kept the same as the present day, but the seasonal distribution has been shifted to more winter-dominated with no snow, as is indicated by the literature discussed above. Under this scenario, average annual lake water values are lower than the present day model (−2.81‰), and could be even more so if annual-averaged precipitation was increased under the same P/E seasonality regime, as seems possible (Roberts et al., 2008). This demonstrates that the seasonality of P/E, in addition to the average annual conditions, is important in controlling inter-annual changes in  $\delta^{18}\text{O}_{\text{lakewater}}$ .

To investigate further the relative contributions of precipitation and temperature (linked closely to evaporation in this model), an early Holocene scenario, using modern day temperatures (as well as modern day annual-average precipitation levels again) and changing only the seasonal distribution of precipitation, was also undertaken. Here  $\delta^{18}\text{O}_{\text{lakewater}}$  was still lower than the present day scenario (−0.57‰) and the average of

monthly P/E increases (Table 2). This result drives a difference in this model because groundwater inflow and outflow are dependent on P/E, with additional groundwater outflow required in the early Holocene compared to present day to balance the lake system, and suggesting higher lake levels under early Holocene conditions. This indicates that changing the seasonal distribution of P/E, irrespective of annual average conditions, can lead to changes in both lake hydrology and lake isotope composition. It highlights the need to be careful when suggesting that the early Holocene was ‘wetter’ than the mid and late Holocene based solely on evidence from lake sediment isotopes, as now it is clear that changes in the seasonality of P/E have an impact on  $\delta^{18}\text{O}$ , in part due to changes in seasonal water balance as well as due to changes in  $\delta^{18}\text{O}$  of precipitation (Table 2), as suggested by Stevens et al. (2001, 2006) for Lakes Zeribar and Mirabad.

## 5.2 *The mid Holocene (~6,500 to ~1,600 years BP)*

At Nar Gölü, a number of proxies respond to changes in lake level, usually driven by changes in P/E, such as lithology (varved vs. non-varved), carbonate mineralogy (calcite vs. aragonite and dolomite) (Dean et al., 2015b), the Sr-Ca elemental ratio and certain diatom species (Roberts et al., 2016). These multiple proxies indicate that annual average P/E was probably lower after ~6,500 years BP compared to the early Holocene.

We know at Nar Gölü that lake level falls lead to more positive  $\delta^{18}\text{O}_{\text{carbonate}}$  (Dean et al., 2015a) and therefore a significant part of the  $\delta^{18}\text{O}$  trend in carbonates and diatoms to higher values in the mid and late Holocene, compared to the early Holocene, is likely related to a shift to drier conditions. Other influences on  $\delta^{18}\text{O}$ , such as changes in the isotopic composition of the source of precipitation, amount effect or temperature, could not have accounted for the large size of the shift in both  $\delta^{18}\text{O}_{\text{carbonate}}$  and  $\delta^{18}\text{O}_{\text{diatom}}$  from the early to mid and late Holocene.

$\Delta\delta^{18}\text{O}_{\text{lakewater}}$  does not initially increase in the mid Holocene because both  $\delta^{18}\text{O}_{\text{carbonate}}$  and  $\delta^{18}\text{O}_{\text{diatom}}$  increase, but in the period ~4,100 to ~1,600 years BP  $\delta^{18}\text{O}_{\text{lakewater}}$  at the time of diatom growth is up to ~4‰ lower than at the time of carbonate precipitation (Figure 4). Annual average precipitation must have been lower for most of the mid and late Holocene compared to the early Holocene (Jones et al., 2007). It is possible that a significant share of this precipitation decline occurred ~7,500 years BP, while at ~4,100 years BP there was a rise in summer evaporation but winter/spring precipitation levels did not change substantially. If that was the case, that would explain why both  $\delta^{18}\text{O}_{\text{diatom}}$  (responding more to winter/spring precipitation) and  $\delta^{18}\text{O}_{\text{carbonate}}$  (responding more to summer evaporation) increased ~7,500 years BP but only  $\delta^{18}\text{O}_{\text{carbonate}}$  increased at ~4,100 years BP (thus leading to increased  $\Delta\delta^{18}\text{O}_{\text{lakewater}}$ ). However, lake level change could account for some of this increased  $\Delta\delta^{18}\text{O}_{\text{lakewater}}$ .  $\Delta\delta^{18}\text{O}_{\text{lakewater}}$  will be more

sensitive to inputs and outputs when the lake level and volume were lower, with less of a buffering effect than when the lake level is higher: this is a well-known phenomenon in limnology (e.g. Leng and Anderson, 2003; Steinman et al., 2010).

To test this with the lake isotope mass balance model, two model conditions are set for this period. In both, precipitation is reduced compared to the present day as multi-proxy evidence from Nar Gölü (Dean et al., 2015b; Roberts et al., 2016) and elsewhere in the region (Roberts et al., 2008) points to lower lake levels at this time. In the first Mid Holocene scenario (MHi), temperatures are held the same as the present day, resulting in an average  $\delta^{18}\text{O}_{\text{lakewater}}$  value of +1.06‰, which is higher than the early Holocene scenarios and thus supports our contention that some of the increase in  $\delta^{18}\text{O}$  could be due to reduced annual precipitation. However, the range in the model is only 1.10‰ (Table 2), which is similar to the early Holocene model, despite the higher  $\Delta\delta^{18}\text{O}_{\text{lakewater}}$  seen in the data in the mid Holocene compared to the early Holocene. In the second Mid Holocene scenario (MHii), summer temperatures are raised to increase summer evaporation such that P/E seasonality is increased relative to MHi. Average  $\delta^{18}\text{O}_{\text{lakewater}}$  values become even more positive (+2.00‰) and the range increases (1.22‰; Table 2). Further, a shift from a steady state lake with the same volume as the present day scenario, in MHii conditions, to one with a 20% smaller volume, increases the intra-



annual  $\delta^{18}\text{O}_{\text{lakewater}}$  range to 1.52‰, showing how a change to lower lake levels could account for some of the increase in  $\Delta\delta^{18}\text{O}_{\text{lakewater}}$  at this time (as discussed above).

To ensure steady state lakes under the mid Holocene climatic scenarios, the groundwater outflow constant has to be reduced (see Supplementary Information for model details). In the model, this is partly a function of P/E as more water entering the lake will push more of it out, however here it needs to be further reduced relative to present day to ensure a steady state lake, i.e. one where volume is not always increasing or decreasing at an annual time step. This suggests there are further controls on groundwater outflow that are not described by our simple model, possibly linked to lake volume and depth, with the lower lake levels of the mid Holocene also potentially contributing to reduced groundwater outflow at these times.

### 5.2.3 Late Holocene (last 1,600 years)

Around 1,600-1,200 years BP,  $\Delta\delta^{18}\text{O}_{\text{lakewater}}$  was at times >10‰. Dean et al. (2013) hypothesised that this was due to a seasonal freshwater lid of low  $\delta^{18}\text{O}$  snowmelt occurring at this time, in which the diatoms lived. To further investigate the sensitivity of the Nar Gölü system to snow volume, the modern lake isotope mass balance model was altered to have no snow, or double the amount of snow, keeping all other variables

the same. This produced more positive or more negative annual average  $\delta^{18}\text{O}_{\text{lakewater}}$  values respectively, as would be expected by putting less or more negative  $\delta^{18}\text{O}$  water into the system (Table 2). There is no impact on the range if these changes are made into a well-mixed lake system as in the model, further suggesting that density differences and stratification are probably important in explaining the  $\Delta\delta^{18}\text{O}_{\text{lakewater}}$  variability reconstructed down-core at Nar Gölü as proposed by Dean et al. (2013) for this unusual period during the late Holocene.

## 6 Conclusions

The combination of two  $\delta^{18}\text{O}$  records, from diatoms and endogenic carbonate that formed in Nar Gölü in central Turkey at different times of the year, helps to inform discussion of palaeoseasonality. Our record indicates that there are three lake states through the Holocene: the early Holocene and the last 1,000 years when there is limited  $\Delta\delta^{18}\text{O}_{\text{lakewater}}$ , the mid Holocene and up to ~1,600 years BP when  $\Delta\delta^{18}\text{O}_{\text{lakewater}}$  was at times ~4‰ and a short period ~1,600-1,200 years BP when  $\Delta\delta^{18}\text{O}_{\text{lakewater}}$  was ~10‰. Modelling results indicate that the increase in  $\Delta\delta^{18}\text{O}_{\text{lakewater}}$  from the early to the mid Holocene could be related to changes in P/E seasonality, but a shift to lower lake levels (and volumes) would have amplified the impact of any changes in P/E. Therefore, while we have shown that using  $\Delta\delta^{18}\text{O}_{\text{lakewater}}$  to compare lake conditions at different

times of the year can provide insights into seasonality, it is not a simple proxy for intra-annual P/E variability. In terms of inter-annual  $\delta^{18}\text{O}$  change, we suggest that lower  $\delta^{18}\text{O}_{\text{carbonate}}$  and  $\delta^{18}\text{O}_{\text{diatom}}$  values in the early Holocene compared to the present day could partly be the result of changes in the seasonality of P/E. However, the multi-proxy evidence available from Nar Gölü clearly points to a mid Holocene transition to lower lake levels driven by annual-mean shifts to reduced P/E.

## Acknowledgments

JRD was funded by NERC PhD studentship NE/I528477/1 (2010-2014). Diatom isotope work was funded by NIGFSC grant IP/1346/1112 to MDJ. Fieldwork was supported by National Geographic and British Institute at Ankara grants to CNR. All authors have contributed intellectually and approved the final version. We would like to thank those others who contributed to field work in 2010 at Nar Gölü: Samantha Allcock, Hakan Yiğitbaşıoğlu, Fabien Arnaud, Emmanuel Malet, Ersin Ateş, Çetin Şenkul, Gwyn Jones, Ryan Smith and Ceran Şekeryapan. George Swann is thanked for his useful advice with the diatom isotope corrections. We thank Gianni Zanchetta and an anonymous reviewer for helpful comments that improved the manuscript. A Supplementary Information file and a data file are associated with the online version of this paper.

## References

- Bar-Yosef Mayer DE, Leng MJ, Aldridge DC, Arrowsmith C, Gumus BA and Sloane HJ (2012) Modern and early-middle Holocene shells of the freshwater mollusc *Unio*, from Catalhoyuk in the Konya Basin, Turkey: preliminary palaeoclimatic implications from molluscan isotope data. *Journal of Archaeological Science* 39: 76-83.
- Beck L, Gehlen M, Flank AM, Van Bennekom AJ and Van Beusekom JEE (2002) The relationship between Al and Si in biogenic silica as determined by PIXE and XAS. *Nuclear Instruments & Methods in Physics Research Section B - Beam Interactions with Materials and Atoms* 189: 180-184.
- Boyer P, Roberts N and Baird D (2006) Holocene environment and settlement on the Çarşamba alluvial fan, South Central Turkey: Integrating Geoarchaeology and Archaeological Field Survey. *GeoArchaeology* 21: 675-699.
- Brayshaw D, Hoskins B and Black E (2010) Some physical drivers of change in the winter storm tracks over the Atlantic and Mediterranean during the Holocene. *Philosophical Transactions of the Royal Society of London* 368: 5185-5223.
- Chapligin B, Leng MJ, Webb E, Alexandre A, Dodd JP, Ijiri A, Lücke A, Shemesh A, Abelman A, Herzschuh U, Longstaffe FJ, Meyer H, Moschen R, Okazaki Y,

- 518 Rees NH, Sharp ZD, Sloane HJ, Sonzogni C, Swann GEA, Sylvestre F, Tyler JJ  
 519 and Yam R (2011) Inter-laboratory comparison of oxygen isotope compositions  
 520 from biogenic silica. *Geochimica et Cosmochimica Acta* 75: 7242-7256.
- 521 Crespín J, Sylvestre F, Alexandre A, Sonzogni C, Pailles C and Perga ME (2010) Re-  
 522 examination of the temperature-dependent relationship between delta O-  
 523 18(diatoms) and delta O-18(lake water) and implications for paleoclimate  
 524 inferences. *Journal of Paleolimnology* 44: 547-557.
- 525 Darling WG, Bath AH, Gibson JJ and Rozanski K (2006) Isotopes in Water. In: Leng  
 526 MJ (ed) *Isotopes in Palaeoenvironmental Research*. Dordrecht: Springer.
- 527 Dean JR, Eastwood WJ, Roberts CN, Jones MD, Yigitbasioglu H, Allcock SL,  
 528 Woodbridge J, Metcalfe SE and Leng MJ (2015a) Tracking the hydro-climatic  
 529 signal from lake to sediment: a field study from central Turkey. *Journal of*  
 530 *Hydrology* 529: 608-621.
- 531 Dean JR, Jones MD, Leng MJ, Noble SR, Metcalfe SE, Sloane HJ, Sahy D, Eastwood  
 532 WJ and Roberts CN (2015b). Eastern Mediterranean hydroclimate over the late  
 533 glacial and Holocene, reconstructed from the sediments of Nar lake, central  
 534 Turkey, using stable isotopes and carbonate mineralogy. *Quaternary Science*  
 535 *Reviews* 124: 162-174.
- 536 Dean JR, Jones MD, Leng MJ, Sloane HJ, Roberts CN, Woodbridge J, Swann GEA,  
 537 Metcalfe SE, Eastwood WJ and Yigitbasioglu H (2013) Palaeo-seasonality of the

- 538 last two millennia reconstructed from the oxygen isotope composition of  
 539 carbonates and diatom silica from Nar Gölü, central Turkey. *Quaternary Science*  
 540 *Reviews* 66: 35-44.
- 541 Djamali M, Akhani H, Andrieu-Ponel V, Braconnot P, Brewer S, de Beaulieu JL,  
 542 Fleitmann D, Fleury J, Gasse F, Guibal F, Jackson ST, Lezine AM, Medail F,  
 543 Ponel P, Roberts N and Stevens L (2010) Indian Summer Monsoon variations  
 544 could have affected the early-Holocene woodland expansion in the Near East. *The*  
 545 *Holocene* 20: 813-820.
- 546 Emeis KC, Struck U, Schulz HM, Rosenberg R, Bernasconi S, Erlenkeuser H,  
 547 Sakamoto T and Martinez-Ruiz F (2000) Temperature and salinity variations of  
 548 Mediterranean Sea surface waters over the last 16,000 years from records of  
 549 planktonic stable oxygen isotopes and alkenone unsaturation ratios.  
 550 *Palaeogeography Palaeoclimatology Palaeoecology* 158: 259-280.
- 551 England A, Eastwood WJ, Roberts CN, Turner R, Haldon JF (2008) Historical  
 552 landscape change in Cappadocia (central Turkey): a palaeoecological  
 553 investigation of annually laminated sediments from Nar lake. *The Holocene* 18:  
 554 1229-1245.
- 555 Gevrek A and Kazanci N (2000) A Pleistocene, pyroclastic-poor maar from central  
 556 Anatolia, Turkey: influence of a local fault on a phreatomagmatic eruption. *Journal*  
 557 *of Volcanology and Geothermal Research* 95: 309-317

- 558 Grossman EL and Ku TL (1986) Oxygen and carbon isotope fractionation in biogenic  
559 aragonite - temperature effects. *Chemical Geology* 59: 59-74.
- 560 Issar A and Adar E (2010) Progressive development of water resources in the Middle  
561 East for sustainable water supply in a period of climate change. *Philosophical*  
562 *Transactions of the Royal Society A - Mathematical Physical and Engineering*  
563 *Sciences* 368: 5339-5350.
- 564 Jones MD, Cuthbert MO, Leng MJ, McGowan S, Mariethoz G, Arrowsmith C, Sloane  
565 HJ, Humphrey KK and Cross I (2016) Comparisons of observed and modelled  
566 lake  $\delta^{18}\text{O}$  variability. *Quaternary Science Reviews* 131: 329-340.
- 567 Jones MD and Imbers J (2010) Modelling Mediterranean lake isotope variability.  
568 *Global and Planetary Change* 71: 193-200.
- 569 Jones MD, Leng MJ, Roberts CN, Turkes M and Moyeed R (2005) A coupled  
570 calibration and modelling approach to the understanding of dry-land lake oxygen  
571 isotope records. *Journal of Paleolimnology* 34: 391-411.
- 572 Jones MD and Roberts CN (2008) Interpreting lake isotope records of Holocene  
573 environmental change in the Eastern Mediterranean. *Quaternary International* 181: 32-  
574 38.
- 575 Jones MD, Roberts CN and Leng MJ (2007) Quantifying climatic change through the  
576 last glacial-interglacial transition based on lake isotope palaeohydrology from  
577 central Turkey. *Quaternary Research* 67: 463-473.

- 578 Jones MD, Roberts CN, Leng MJ and Türkeş M (2006) A high-resolution late Holocene  
579 lake isotope record from Turkey and links to North Atlantic and monsoon climate.  
580 *Geology* 34: 361-364.
- 581 Kelley CP, Mohtadi S, Cane MA, Seager R and Kushnir Y (2015) Climate change in  
582 the Fertile Crescent and implications of the recent Syrian drought. *Proceedings of*  
583 *the National Academy of Sciences* 112: 3241-3246.
- 584 Kim ST and O'Neil JR (1997) Equilibrium and nonequilibrium oxygen isotope effects  
585 in synthetic carbonates. *Geochimica et Cosmochimica Acta* 61: 3461-3475.
- 586 Koning E, Gehlen M, Flank AM, Calas G and Epping E (2007) Rapid post-mortem  
587 incorporation of aluminum in diatom frustules: evidence from chemical and  
588 structural analyses. *Marine Chemistry* 106: 208-222.
- 589 Kotthoff U, Prodd J, Müller UC, Peyron O, Schmiedl G, Schulz H and Bordon A (2008)  
590 Climate dynamics in the borderlands of the Aegean Sea during formation of  
591 sapropel S1 deduced from a marine pollen record. *Quaternary Science Reviews*  
592 27: 832-845.
- 593 Kutiel H and Türkeş M (2005) New evidence for the role of the North Sea-Caspian  
594 Pattern on the temperature and precipitation regimes in continental Central  
595 Turkey. *Geografiska Annaler Series A - Physical Geography* 87A: 501-513.
- 596 Leng MJ and Anderson AJ (2003) Isotopic variation in modern lake waters from  
597 western Greenland. *The Holocene* 13: 605-611. Leng MJ and Sloane HJ (2008).



- 598 Combined oxygen and silicon isotope analysis of biogenic silica. *Journal of*  
 599 *Quaternary Science* 23: 313-319.
- 600 Lewis JP, Leng MJ, Dean JR, Marciniak A, Bar-Yosef Mayer DE and Wu X (2017)  
 601 Early Holocene palaeoseasonality inferred from the stable isotope composition of  
 602 Unio shells from Çatalhöyük, Turkey. *Environmental Archaeology* 1: 79-95.
- 603 Mackay AW, Swann GEA, Brewer TS, Leng MJ, Morley DW, Piotrowska N, Rioual P.  
 604 and White D (2011) A reassessment of late glacial-Holocene diatom oxygen  
 605 isotope record from Lake Baikal using a geochemical mass-balance approach.  
 606 *Journal of Quaternary Science* 26: 627-634.
- 607 McGarry S, Bar-Matthews M, Matthews A, Vaks A, Schilman B and Ayalon A (2004)  
 608 Constraints on hydrological and paleotemperature variations in the Eastern  
 609 Mediterranean region in the last 140 ka given by the delta D values of speleothem  
 610 fluid inclusions. *Quaternary Science Reviews* 23: 919-934.
- 611 Morley DW, Leng MJ, Mackay AW, Sloane HJ, Rioual P and Battarbee RW (2004)  
 612 Cleaning of lake sediment samples for diatom oxygen isotope analysis. *Journal of*  
 613 *Paleolimnology* 31: 391-401.
- 614 Peyron O, Combourieu-Nebout N, Brayshaw D, Goring S, Andrieu-Ponel V, Desprat S,  
 615 Fletcher W, Gambin B, Ioakim C, Joannin S, Kotthoff U, Kouli K, Montade V,  
 616 Pross J, Sadori L and Magny M (2017). Precipitation changes in the

- 617 Mediterranean basin during the Holocene from terrestrial and marine pollen  
 618 records: a model-data comparison. *Climate of the Past* 13: 249-265.
- 619 Peyron O, Goring S, Dormoy I, Kotthoff U, Pross J, De Beaulieu JL, Drescher-  
 620 Schneider R, Vanniere B and Magny M (2011) Holocene seasonality changes in  
 621 the central Mediterranean region reconstructed from the pollen sequences of Lake  
 622 Accesa (Italy) and Tenaghi Philippon (Greece). *The Holocene* 21: 131-146.
- 623 Ren H, Brunelle BG, Sigman DM and Robinson RS (2013) Diagenetic aluminum  
 624 uptake into diatom frustules and the preservation of diatom-bound organic  
 625 nitrogen. *Marine Chemistry* 155: 92-101.
- 626 Roberts CN, Allcock SL, Arnaud F, Dean JR, Eastwood WJ, Jones MD, Leng MJ,  
 627 Metcalfe SE, Malet E, Woodbridge J and Yiğitbaşıoğlu H (2016) A tale of two  
 628 lakes: a multi-proxy comparison of Late Glacial and Holocene environmental  
 629 change in Cappadocia, Turkey. *Journal of Quaternary Science* 31: 348-362.
- 630 Roberts N, Jones MD, Benkaddour A, Eastwood WJ, Filippi ML, Frogley MR, Lamb  
 631 HF, Leng MJ, Reed JM, Stein M, Stevens L, Valero-Garces B and Zanchetta G  
 632 (2008) Stable isotope records of Late Quaternary climate and hydrology from  
 633 Mediterranean lakes: the ISOMED synthesis. *Quaternary Science Reviews* 27:  
 634 2426-2441.
- 635 Roberts N, Reed JM, Leng MJ, Kuzucuoğlu C, Fontugne M, Bertaux J, Woldring H,  
 636 Bottema S, Black S, Hunt, E and Karabiyikoglu M (2001) The tempo of Holocene

- 637 climatic change in the eastern Mediterranean region: new high-resolution crater-  
638 lake sediment data from central Turkey. *The Holocene* 11: 721-736.
- 639 Rohling EJ (2016) Of lakes and fields: A framework for reconciling palaeoclimatic  
640 drought inferences with archaeological impacts. *Journal of Archaeological*  
641 *Science* 73: 17-24.
- 642 Rossignol-Strick M (1999) The Holocene climatic optimum and pollen records of  
643 sapropel 1 in the eastern Mediterranean, 9000-6000 BP. *Quaternary Science*  
644 *Reviews* 18: 515-530.
- 645 Steinman BA, Rosenmeier MF and Abbott MB (2010) The isotopic and hydrologic  
646 response of small, close-basin lakes to climate forcing from predictive models:  
647 simulations of stochastic and mean state precipitation variations. *Limnology and*  
648 *Oceanography* 55: 2246-2261.
- 649 Stevens LR, Ito E, Schwalb A and Wright HE (2006) Timing of atmospheric  
650 precipitation in the Zagros Mountains inferred from a multi-proxy record from  
651 Lake Mirabad, Iran. *Quaternary Research* 66: 494-500.
- 652 Stevens LR, Wright HE and Ito E (2001) Proposed changes in seasonality of climate  
653 during the Lateglacial and Holocene at Lake Zeribar, Iran. *The Holocene* 11: 747-  
654 755.

- 655 Swann GEA (2010) A comparison of the Si/Al and Si/time wet-alkaline digestion  
656 methods for measurement of biogenic silica in lake sediments. *Journal of*  
657 *Paleolimnology* 44: 375-385.
- 658 Swann GEA and Leng MJ (2009) A review of diatom delta O-18 in palaeoceanography.  
659 *Quaternary Science Reviews* 28: 384-398.
- 660 Triantaphyllou MV, Ziveri P, Gogou A, Marino G, Lykousis V, Bouloubassi I, Emeis  
661 KC, Kouli K, Dimiza M, Rosell-Mele A, Papanikolaou M, Katsouras G and  
662 Nunez N (2009) Late Glacial-Holocene climate variability at the south-eastern  
663 margin of the Aegean Sea. *Marine Geology* 266: 182-197.
- 664 Turner R, Roberts N, Eastwood WJ, Jenkins E and Rosen A (2010) Fire, climate and the  
665 origins of agriculture: micro-charcoal records of biomass burning during the last  
666 glacial-interglacial transition in Southwest Asia. *Journal of Quaternary Science*  
667 25: 371-386.
- 668 Turner R, Roberts N and Jones MD (2008) Climatic pacing of Mediterranean fire  
669 histories from lake sedimentary microcharcoal. *Global and Planetary Change* 63:  
670 317-324.
- 671 Tyler JJ, Leng MJ and Sloane HJ (2007) The effects of organic removal treatment on  
672 the integrity of delta O-18 measurements from biogenic silica. *Journal of*  
673 *Paleolimnology* 37: 491-497.

- 674 Vanniere B, Power MJ, Roberts N, Tinner W, Carrion J, Magny M, Bartlein P,  
 675 Colombaroli D, Danialu AL, Finsinger W, Gil-Romera G, Kaltenrieder P, Pini R,  
 676 Sadori L, Turner R, Valsecchi V and Vescovi E (2011) Circum-Mediterranean  
 677 fire activity and climate changes during the mid-Holocene environmental  
 678 transition (8500-2500 cal. BP). *The Holocene* 21: 53-73.
- 679 Weiss H, Courty M-A, Wetterstrom W, Guichard F, Senior L, Meadow R and Curnow  
 680 A (1993) The genesis and collapse of third millennium north Mesopotamian  
 681 civilization. *Science* 261: 995-1004.
- 682 Wick L, Lemcke G and Sturm M (2003) Evidence of Lateglacial and Holocene climatic  
 683 change and human impact in eastern Anatolia: high-resolution pollen, charcoal,  
 684 isotopic and geochemical records from the laminated sediments of Lake Van,  
 685 Turkey. *The Holocene* 13: 665-675.
- 686 Woldring H and Bottema S (2003) The vegetation history of East-Central Anatolia in  
 687 relation to Archaeology: the Eski Acigol pollen evidence compared with the Near  
 688 Eastern environment. *Palaeohistoria* 43/44: 1-34.
- 689 Woodbridge J and Roberts CN (2010) Linking neo- and palaeolimnology: a case study  
 690 using crater lake diatoms from central Turkey. *Journal of Paleolimnology* 44:  
 691 855-871.

692 Woodbridge J and Roberts CN (2011) Late Holocene climate of the Eastern  
693 Mediterranean inferred from diatom analysis of annually-laminated lake  
694 sediments. *Quaternary Science Reviews* 30: 3381-3392.  
695

696 **Table 1** Sources of uncertainty associated with the correction of  $\delta^{18}\text{O}_{\text{diatom}}$  data used in  
 697 this paper.

Source of uncertainty	Magnitude of uncertainty
Diatom isotope measurement analytical reproducibility ( $1\sigma$ )	0.3‰
$\text{Al}_2\text{O}_3$ measurement analytical reproducibility ( $1\sigma$ )	0.03%
Variance in $\text{Al}_2\text{O}_3$ composition of turbidites (from $\bar{x}$ of 14.56%) ( $1\sigma$ )	1.6%
Variance in $\delta^{18}\text{O}$ value of turbidites from $\bar{x}$ of 16.0‰ ( $1\sigma$ )	1.0‰

698

699

**Table 2** Lake isotope mass balance model summary

	$\delta l$ (‰)		Tav (°C)	P (mm)	$\delta p$ (‰)	Qi average	Qo average	Volume	P/E
	Mean	Range	Mean	Total	Weighted Mean	(m <sup>3</sup> /month)	(m <sup>3</sup> /month)	(m <sup>3</sup> )	Annual average
Modern	0.59	1.06	11.7	356.2	−9.4	76328	39812	7500000	0.422
with no snow	0.71	1.05	11.7	356.2	−8.5	76328	39812	7500000	0.422
with double snow	0.50	1.06	11.7	356.2	−10.4	76328	39812	7500000	0.422
Mid Holocene i	1.06	1.10	11.7	295.2	−8.8	71991	32851	7500000	0.398
Mid Holocene ii	2.00	1.22	12.6	295.2	−8.8	70781	25635	7500000	0.391
	2.00	1.52	12.6	295.2	−8.8	70781	25635	6000000	0.391
Early Holocene	−2.81	1.19	10.7	356.2	−8.9	116438	86320	7500000	0.643
	−2.81	0.99	10.7	356.2	−8.9	116438	86320	9000000	0.643
with modern temperatures	−0.57	1.21	11.7	356.2	−8.9	90813	54422	7500000	0.502



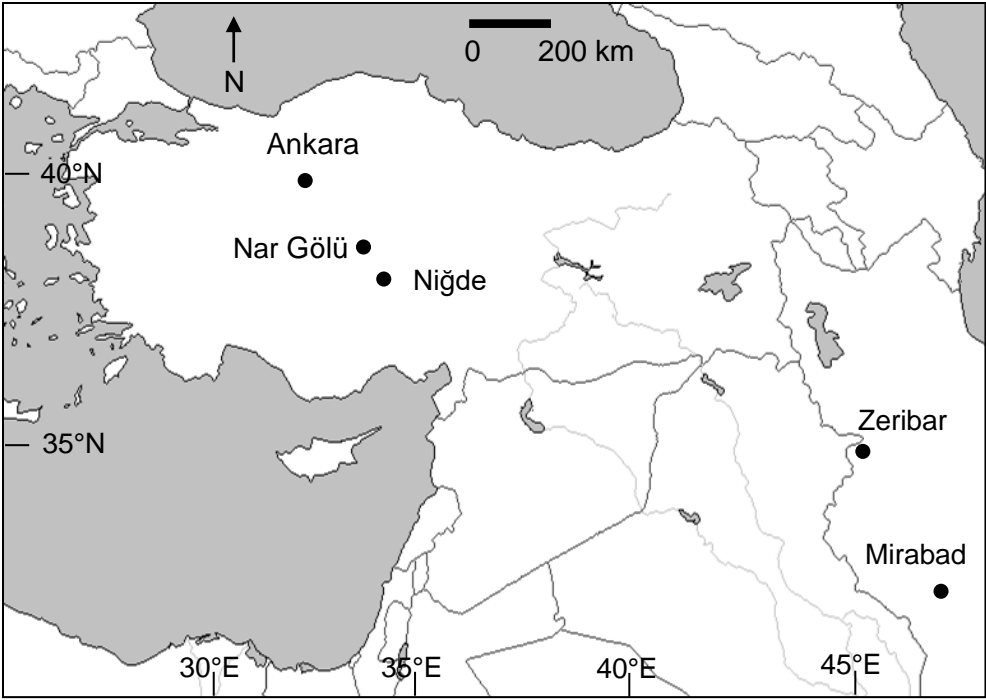
## Figure captions

**Figure 1** Location of Nar Gölü in Turkey and lakes Zeribar and Mirabad in Iran.

**Figure 2** Seasonal data from 2011-2012, showing increase in lake water  $\delta^{18}\text{O}$  (A) and temperature (B) between the estimated times of year of diatom growth (i) and carbonate formation (ii).

**Figure 3**  $\delta^{18}\text{O}_{\text{diatom}}$  and  $\delta^{18}\text{O}_{\text{carbonate}}$  data plotted against depth, with the error bars on  $\delta^{18}\text{O}_{\text{diatom}}$  representing the combined uncertainties from Table 1. There are no carbonate isotope data in sections where there were gaps due to coring (shown by white boxes on the lithology plot) or where there were high levels (>20%) of dolomite (explained in detail in Dean et al., 2015b). Gaps in the diatom isotope data are due to gaps in coring or insufficient amounts of diatom silica.

**Figure 4** (A)  $\delta^{18}\text{O}_{\text{carbonate}}$  (with carbonate mineralogy data) and (B)  $\delta^{18}\text{O}_{\text{diatom}}$ , with (C) data converted to  $\delta^{18}\text{O}_{\text{lakewater}}$  assuming a temperature range of +15 to +20°C for the time of carbonate precipitation and +5 to +10°C for the time of diatom growth. Some isotope data plotted against depth are not shown against age due to issues with the chronology (discussed in detail in Dean et al., 2015b).



Surface  $\delta^{18}\text{O}_{\text{lakewater}}$   
‰ VSMOW

A

0

-1

-2

Increase of  
 $\sim 0.5\text{‰}$

B

Increase of  
 $\sim 10^{\circ}\text{C}$

01/06/2011

01/09/2011

02/12/2011

03/03/2012

03/06/2012

Date

Daily average water T at  
5 m depth  $^{\circ}\text{C}$

25

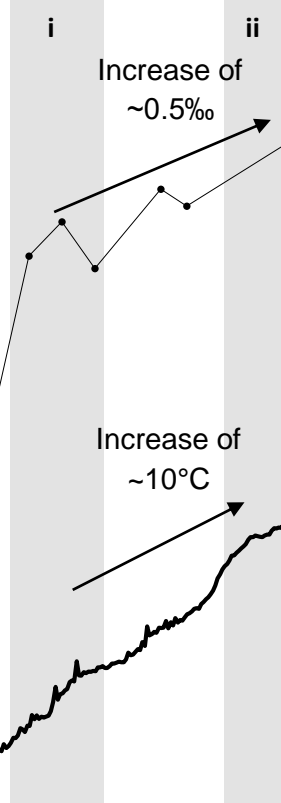
20

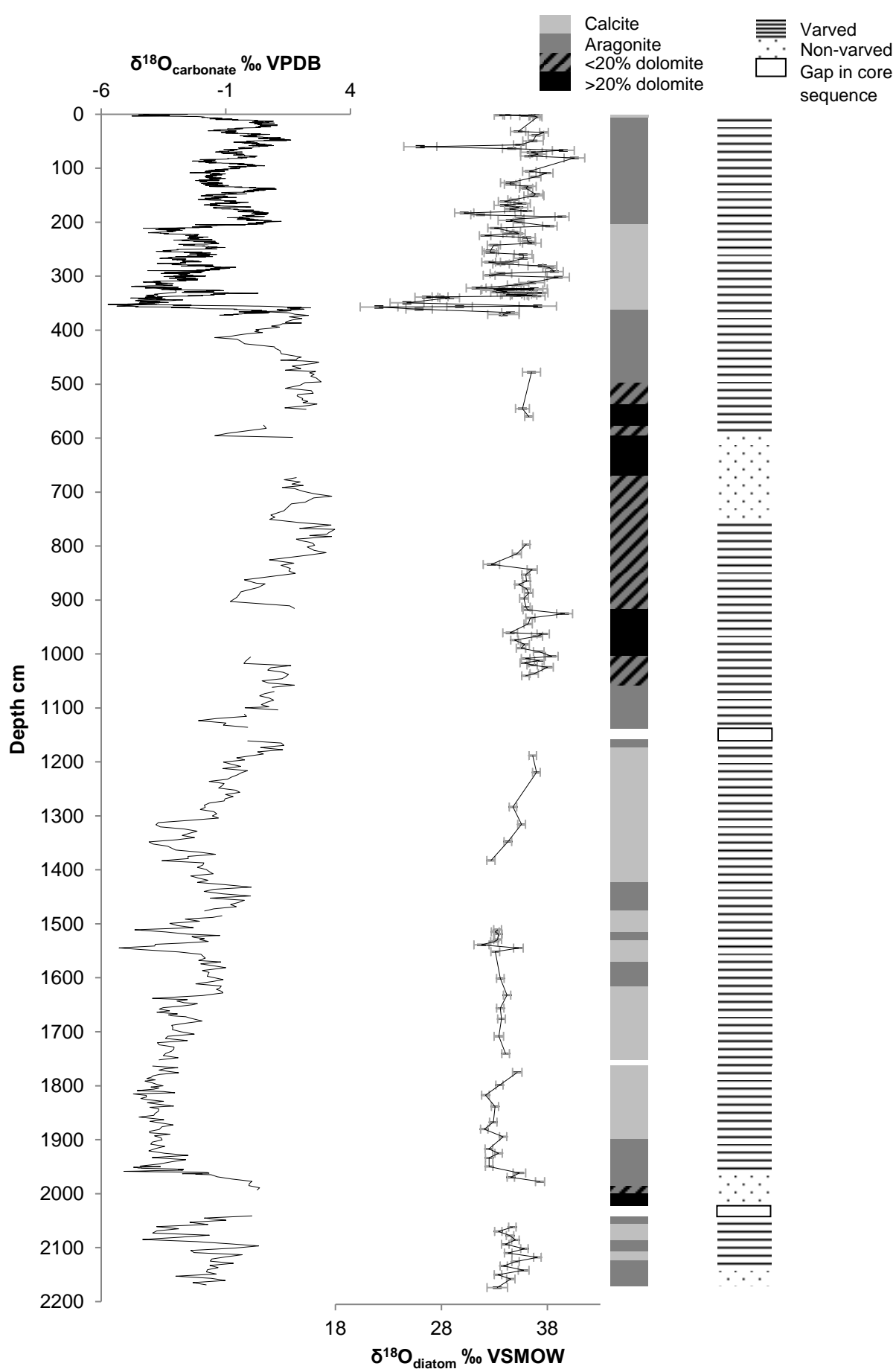
15

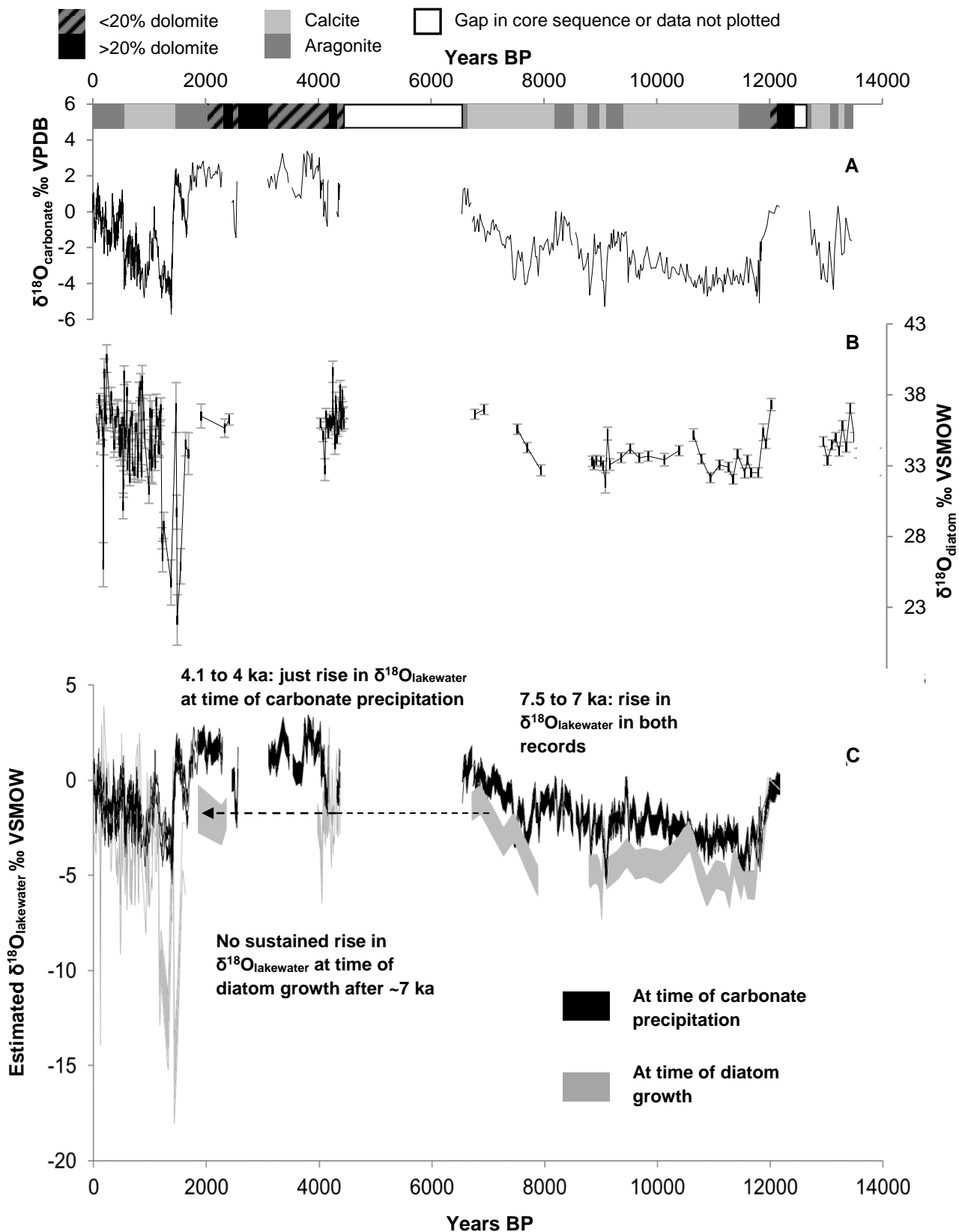
10

5

0







Supplementary Information for Seasonality of Holocene hydroclimate in the Eastern Mediterranean reconstructed using the oxygen isotope composition of carbonates and diatoms from Lake Nar, central Turkey

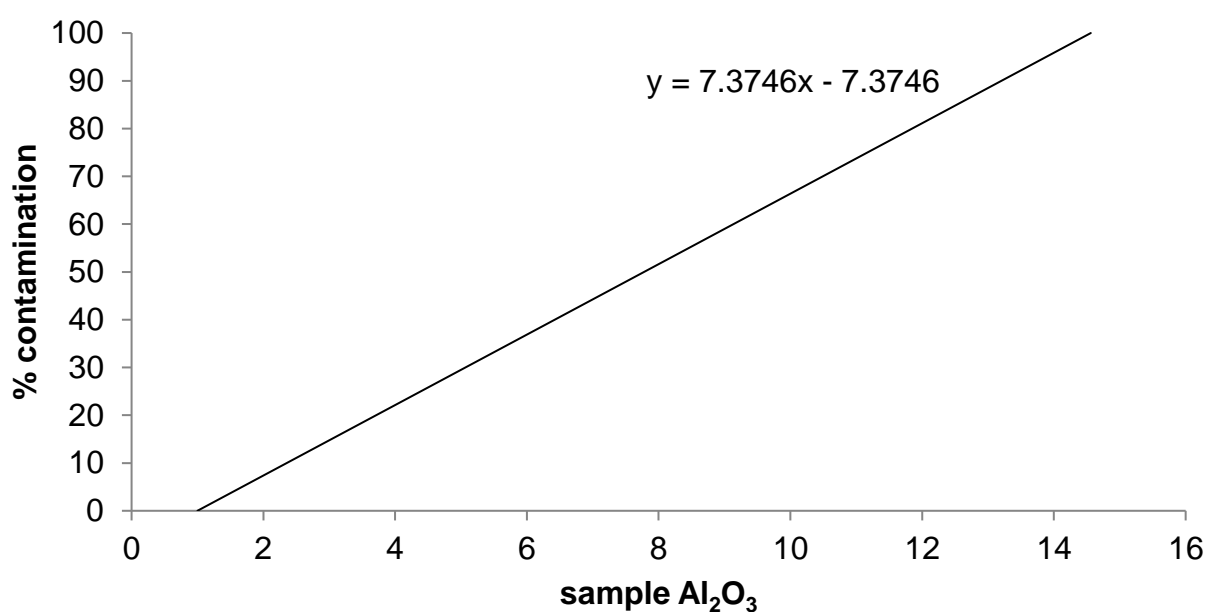


**Figure SI-1** Regression line showing equation used to derive Eq. 2: a mixing line between the point when Al<sub>2</sub>O<sub>3</sub> is 14.56% indicating 100% contamination and when Al<sub>2</sub>O<sub>3</sub> is 1% indicating 0% contamination (i.e. 100% diatom).

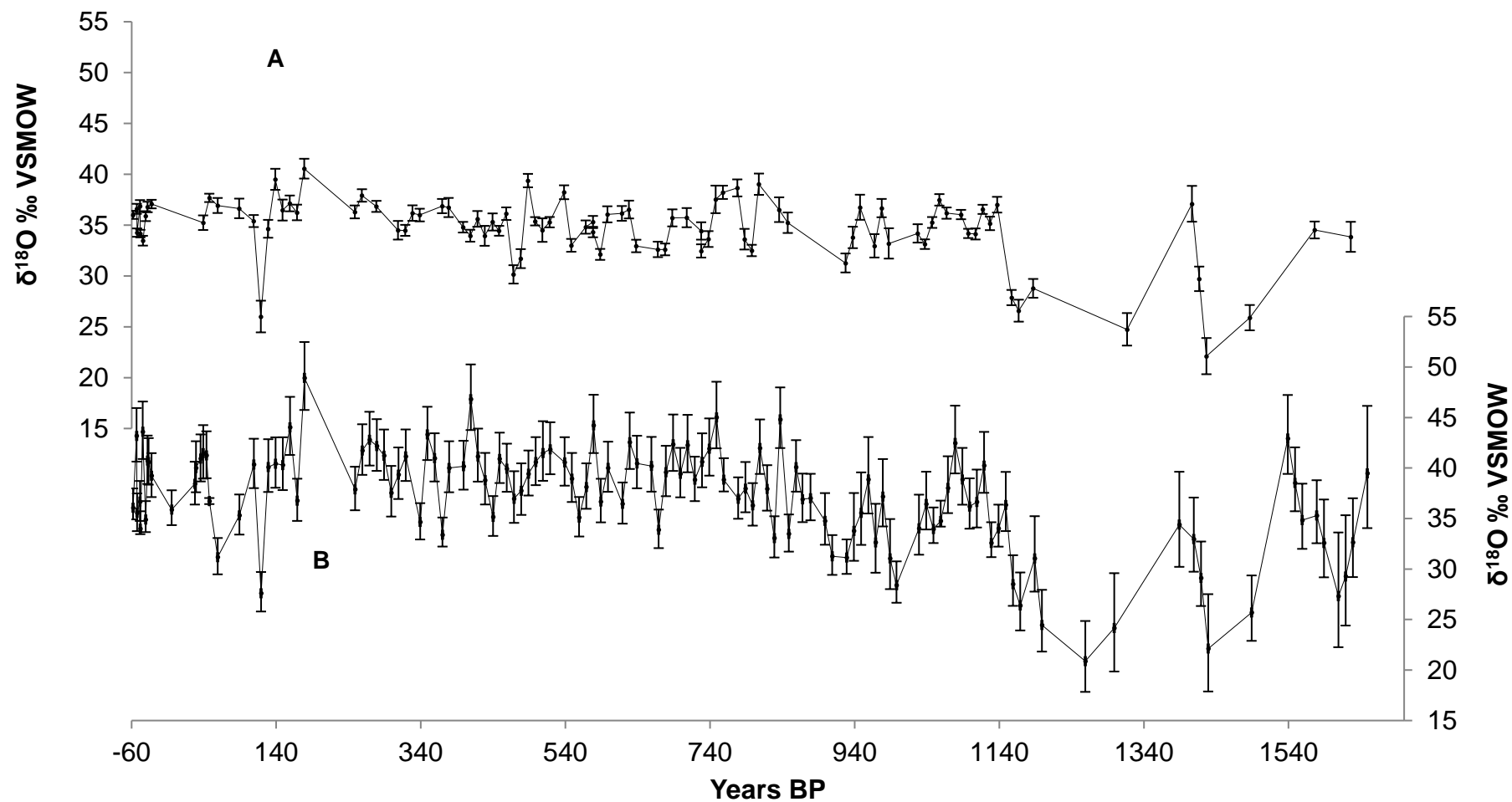


**Figure SI-2** The difference between NAR01/02 diatom isotope trends in this paper (A) and as published in Dean et al. (2013) (B). Not all samples originally run and corrected in B could be included in A because many did not have sufficient material left to allow for XRF analysis. Error bars show the combined uncertainties from the factors given in Table 1.

## **Isotope Mass Balance Models**

### **Theoretical model**

The following is edited from Jones et al. (2016) and Jones and Imbers (2010) for the model lake used in this study.

The water mass and isotopic mass balance of a well-mixed lake is, respectively:

$$\frac{dV}{dt} = P + Qi - E - Qo \quad (1)$$

$$\frac{d}{dt}(V\delta_L) = P\delta_P + Qi\delta_P - E\delta_E - Qo\delta_L \quad (2)$$

where  $V$  is the lake volume,  $t$ , time,  $P$ , precipitation on lake surface per unit time,  $E$  is evaporation from lake surface per unit time and  $Q_o$  and  $Q_i$  are obtained as  $Q_x = S_x + G_x$ , where  $S_o$  and  $G_o$  and  $S_i$  and  $G_i$  are the surface and groundwater outflows and inflows respectively, and are measured in the same units as  $P$  and  $E$ .  $\delta_P$ ,  $\delta_E$  and  $\delta_L$  are the isotope values, either  $\delta^{18}\text{O}$  or  $\delta\text{D}$ , of the precipitation, evaporation and lake waters respectively.

$\delta_E$  is difficult to measure and is therefore usually calculated (e.g. Steinman et al., 2010) using equations based on the evaporation model of Craig and Gordon (1965) such that

$$\delta_E = \frac{\alpha^*\delta_L - h\delta_A - \epsilon}{1 - h + 0.001\epsilon_k} \quad (3)$$

where  $\alpha^*$  is the equilibrium isotopic fractionation factor dependent on the temperature at the evaporating surface and

$$\frac{1}{\alpha^*} = \exp(1137T_L^{-2} - 0.4256T_L^{-1} - 2.0667 \times 10^{-3}) \quad (4)$$

for oxygen and

$$\frac{1}{\alpha^*} = \exp(24844T_L^{-2} - 76.248T_L^{-1} - 52.61 \times 10^{-3}) \quad (5)$$

for hydrogen.  $T_L$  is the temperature of the lake surface water in degrees Kelvin (Majoube 1971).  $h$  is the relative humidity normalised to the saturation vapour pressure at the temperature of the air



water interface and  $\epsilon_k$  is the kinetic fraction factor; for  $\delta^{18}\text{O}$   $\epsilon_k$  has been shown to approximate  $14.2(1-h)$  and  $12.5(1-h)$  for  $\delta^2\text{H}$  (Gonfiantini, 1986).  $\delta_A$  is the isotopic value of the air vapour over the lake and  $\epsilon = \epsilon^* + \epsilon_k$  where  $\epsilon^* = 1000(1-\alpha^*)$ .

In the model we use an equation derived from those above to calculate the isotopic value of lake waters ( $\delta_L$ ) at a given time,  $t+\Delta t$ , based on the value of  $\delta_L$  at time  $t$ , and the inputs and outputs from the lake between  $t$  and  $t + \Delta t$ .

The left-hand side of Eq. 2 is expanded and Eq.1 substituted into it:

$$\frac{d}{dt}(V\delta_L) = V \frac{d\delta_L}{dt} + \delta_L \frac{dV}{dt} = \delta_L(P + Qi - E - Qo) + V \frac{d\delta_L}{dt} \quad (6)$$

and then re-written, such that  $\delta_L$  dependences are explicit.

$\delta_E$  is expressed as a function of  $\delta_L$  such that

$$\delta_E = A\delta_L + C \quad (7)$$

where, for Equation 3

$$A = \frac{\alpha^*}{1-h+0.001\epsilon_k} \text{ and } C = -\frac{h\delta_A+\epsilon}{1-h+0.001\epsilon_K}$$

Taking Eq. (2) and (6) and replacing  $\delta_E$  using Eq. (7):

$$V \frac{d\delta_L}{dt} + \delta_L(P + Qi - E - Qo) = \delta_P(P + Qi) - E(A\delta_L + C) - Qo\delta_L \quad (8)$$

Rearranging all terms in Eq.(8) then leads to:

$$V \frac{d\delta_L}{dt} = \delta_P(P + Qi) - EC - \delta_L(P + Qi - E(1 - A)) \quad (9)$$

We define  $\lambda$  and  $\beta$  as:  $\lambda = (P+Qi) \delta_P - EC$  and  $\beta = P+Qi - E(1-A)$  such that equation (9) can be rewritten as:

$$V \frac{d\delta_L}{dt} = \lambda - \beta \delta_L \quad (10)$$

We assume that  $dV/dt$  can be adequately approximated as equal to the change of volume over 1 month and all other variables are also put into the model as rates per month.

Integrating equation (10) obtains an expression for the evolution of  $\delta_L$  with time. At this stage we introduce a first approximation by assuming a constant value for  $V$  for each month; consistent with constant values of  $P$  and  $Q_i$  etc. over each month. The following parameterisation for  $V$  is used:

$$\bar{V} = \frac{V_{30th} + V_0}{2} \quad (11)$$

where  $V_{30th}$  is the total volume on the last day of each month, and  $V_0$  is the initial volume on the first day of the month.

Integration of Eq. (10) after considering the approximation in equation (11) results in:

$$\ln \left( \frac{\lambda - \beta \delta_{L0}}{\lambda - \beta \delta_L} \right) = \frac{\beta}{\bar{V}} \Delta t \quad (12)$$

Where  $\delta_{L0}$  is the initial isotopic composition (i.e. at the beginning of each month) and  $\Delta t=1$  for each monthly step of our model. Finally exponentials of both sides of Eq. (12) give an expression for  $\delta_L$ :

$$\delta_L = \frac{1}{\beta} (\lambda - (\lambda - \beta \delta_{L0}) \exp(-\frac{\beta}{\bar{V}})) \quad (13)$$

### Values for this model

$T_L$ : temperature of the lake surface water

From monitoring data of Lake Nar (Jones et al., 2005, Dean et al., 2015) and other studies (Jones et al., 2016) lake surface temperatures in the model are taken as the average of mean and maximum air temperatures.

*h: normalised relative humidity*

Relative humidity values were calculated based on present day relationships with temperature (c.f. Jones et al., 2005) such that these values could change in time in palaeo scenarios.

These values were normalised to the conditions at the lake surface using the saturation vapour pressure of the air and surface water as defined in Steinman et al. (2010).

*E: Evaporation*

Evaporation is calculated based on the equation of Linacre (1992) that has been shown previously (Jones et al., 2005; Jones et al., 2007) to be a reasonable measure of evaporation and is especially useful for palaeo-contexts where instrumental measurements are non-existent.

$$E(\text{mm/day}) = [0.015 + 4 \times 10^{-4} T_a + 10^{-6} z] \times [480 (T_a + 0.006z) / (84 - A) - 40 + 2.3 u (T_a - T_d)] \quad (14)$$

where  $T_a$  is air temperature ( $^{\circ}\text{C}$ ),  $z$  = altitude (m),  $A$  = latitude,  $T_d$  = dew point temperature =  $0.52 T_{a \text{ min}} + 0.60 T_{a \text{ max}} - 0.009 (T_{a \text{ max}})^2 - 2^{\circ}\text{C}$ .

*$\delta_P$ : isotopic composition of precipitation*

Values for the isotopic composition of rainfall at Nar came from the Online Isotopes in Precipitation Calculator (Bowen et al., 2005; Bowen, 2016).

Isotopic values of snow were based on sampling of snowfall from the catchment (Dean et al., 2013) and were fixed at  $-15\text{‰}$  (i.e. more negative than rainfall). Monthly values are kept as modern throughout, although the weighted annual mean values change as the amount of precipitation in a given month changes in each scenario (Table 2).

*$Q_i$ : surface and groundwater inflow*

The model lake has no surface inflow; this is similar to Lake Nar where there are no permanent stream inflows to the lake.

Monitoring of springs within the Nar catchment (Jones et al., 2005) has shown these to be meteoric water, such that the isotopic composition of inflowing waters to the model lake are considered to be the same as rainfall.

Values of  $Q_i$  and  $Q_o$  are optimised in the model to allow a stable lake with mean isotope values, and intra-annual range, similar to that of Lake Nar. In this model  $Q_i$  is a function of P:E.

*$Q_o$ : surface and groundwater outflow*

There is no surface run off from the model lake, or from Lake Nar.

The amount of groundwater outflow is optimised for the model as described above and in the model lake is dependent on P:E, as the amount of groundwater inflow will change the flow of water through the lake, and a constant for when  $Q_i$  is potentially 0 such that the lake is balanced.

**Table SI-1: precipitation values (mm) used in models**

Month	Modern			Mid Holocene Rainfall	Early Holocene Rainfall
	Snow	Rainfall	Total		
Jan	17.0	16.2	33.2	40.0	51.0
Feb	15.1	21.7	36.7	36.7	46.0
Mar	7.3	31.1	38.4	30.0	40.0
Apr	2.8	44.5	47.2	25.0	30.0
May		38.8	38.8	20.0	20.0
Jun		21.4	21.4	15.0	10.0
Jul		7.7	7.7	7.0	7.7
Aug		7.3	7.3	7.3	7.3
Sep		17.2	17.2	17.2	17.2
Oct		31.6	31.6	25.0	31.0
Nov	6.5	35.3	41.8	32.0	45.0
Dec	13.4	21.4	34.8	40.0	51.0

**Table SI-2: temperatures for Modern and Mid Holocene I scenarios (°C)**

Month	Average (Tav)	Minimum (Tmin)	Maximum (Tmax)
Jan	0.16	-4.05	5.47
Feb	1.46	-3.08	6.88
Mar	5.92	0.70	11.87
Apr	10.57	4.82	16.54
May	15.88	9.04	22.27
Jun	20.28	12.88	26.62
Jul	23.69	15.83	30.31
Aug	23.41	15.69	30.41
Sep	18.33	11.13	25.85
Oct	12.57	6.72	19.74
Nov	6.37	1.25	13.27
Dec	2.34	-1.93	7.96

**Table SI-3: temperatures for Mid Holocene ii scenario (°C)**

<b>Month</b>	<b>Average (Tav)</b>	<b>Minimum (Tmin)</b>	<b>Maximum (Tmax)</b>
Jan	0.16	-4.05	5.47
Feb	1.46	-3.08	6.88
Mar	5.92	0.70	11.87
Apr	10.57	4.82	16.54
May	17.00	10.00	23.00
Jun	21.50	14.00	28.50
Jul	25.00	17.00	31.50
Aug	25.50	16.50	31.00
Sep	21.50	12.00	25.85
Oct	15.00	7.00	19.74
Nov	6.37	1.25	13.27
Dec	2.34	-1.93	7.96

**Table SI-4: temperatures for Early Holocene ii scenario (°C)**

<b>Month</b>	<b>Average (Tav)</b>	<b>Minimum (Tmin)</b>	<b>Maximum (Tmax)</b>
Jan	0.16	0.00	5.47
Feb	1.46	0.50	6.88
Mar	5.92	0.70	11.87
Apr	10.57	4.82	16.54
May	15.00	9.04	21.00
Jun	18.00	10.00	25.00
Jul	20.00	13.00	28.00
Aug	20.00	13.00	28.00
Sep	17.00	10.00	25.00
Oct	12.57	5.00	18.00
Nov	6.37	3.00	12.00
Dec	2.34	0.00	7.00

## **References for supplementary information**

- Bowen GJ (2016) The Online Isotopes in Precipitation Calculator. Available at: [http://wateriso.utah.edu/waterisotopes/pages/data\\_access/oipc.html](http://wateriso.utah.edu/waterisotopes/pages/data_access/oipc.html) Accessed: 1 August 2016.
- Bowen GJ, Wassenaar LI and Hobson KA (2005) Global application of stable hydrogen and oxygen isotopes to wildlife forensics. *Oecologia* 143: 337-348.
- Craig H and Gordon LI (1965) *Dueterium and oxygen-18 variation in the ocean and marine atmosphere. Stable Isotopes in Oceanography Studies and Paleotemperatures*. Pisa: Laboratory di Geologica Nucleara.
- Dean JR, Eastwood WJ, Roberts CN, Jones MD, Yigitbasioglu H, Allcock SL, Woodbridge J, Metcalfe SE and Leng MJ (2015) Tracking the hydro-climatic signal from lake to sediment: a field study from central Turkey. *Journal of Hydrology* 529: 608-621.
- Dean JR, Jones MD, Leng MJ, Sloane HJ, Roberts CN, Woodbridge J, Swann GEA, Metcalfe SE, Eastwood WJ and Yigitbasioglu H (2013) Palaeo-seasonality of the last two millennia reconstructed from the oxygen isotope composition of carbonates and diatom silica from Nar Gölü, central Turkey. *Quaternary Science Reviews* 66: 35-44.
- Gonfiantini R (1986) Environmental isotopes in lake studies. In: Fritz, P., Fontes, J. (eds). *Handbook of Environmental Isotope Geochemistry*, vol. 3. New York: Elsevier. pp. 113-168.
- Jones MD, Cuthbert MO, Leng MJ, McGowan S, Mariethoz G, Arrowsmith C, Sloane HJ, Humphrey KK and Cross I (2016) Comparisions of observed and modelled lake  $\delta^{18}\text{O}$  variability. *Quaternary Science Reviews* 131: 329-340.
- Jones MD and Imbers J (2010) Modelling Mediterranean lake isotope variability. *Global and Planetary Change* 71: 193-200.

- Jones MD, Leng MJ, Roberts CN, Türkeş M and Moyeed R (2005) A coupled calibration and modelling approach to the understanding of dry-land lake oxygen isotope records. *Journal of Paleolimnology* 34: 391-411.
- Jones MD, Roberts CN and Leng MJ (2007) Quantifying climatic change through the last glacial-interglacial transition based on lake isotope palaeohydrology from central Turkey. *Quaternary Research* 67: 463-473.
- Linacre E (1992) *Climate Data and Resources: a Reference and Guide*. London: Routledge.
- Majoube F (1971) Fractionnement en oxygene-18 et un deuterium entre l'eau et sa vapeur. *Journal of Chemical Physics* 187: 1423-1436.
- Steinman BA, Rosenmeier MF, Abbott MB and Bain DJ (2010) The isotopic and hydrologic response of small, closed-basin lakes to climate forcing from predictive models: application to paleoclimate studies in the upper Columbia River basin. *Limnology and Oceanography* 55: 2231-2245.